



Aerodynamic Analysis of a Conceptual Fixed-Wing Vertical Take-Off and Landing UAV Powered by a Piston Engine

Dafiaghor Aghoghorohenena Gordon, Abdussalam El-Suleiman, Rexcharles Enyinna Donatus, Mathias Usman Bonet, Samuel David Iyaghigba

Aerospace Engineering Department, Air Force Institute of Technology, Kaduna, Nigeria

ABSTRACT

This study presents an aerodynamic analysis of a conceptual fixed-wing vertical take-off and landing (FW-VTOL) unmanned aerial vehicle (UAV) powered by a piston engine. The primary objective was to optimize the lift-to-drag (L/D) ratio to improve the UAV's flight range and aerodynamic efficiency. Using XFLR5 software, the performance of selected airfoils NACA 4412 for the wing and NACA 0011 for the tail was evaluated under varying angles of attack and trim conditions. The analysis identified a maximum L/D ratio of 20.904 between 3.05° and 3.10° angles of attack. A trim angle of 1.847° produced an L/D ratio of 20.150 with a drag coefficient of 0.024, closely matching the minimum drag value of 0.023. These results confirm the aerodynamic efficiency of the selected configuration. Compared to prior studies, which primarily focused on general UAV designs or high-fidelity simulations, this study demonstrates the effectiveness of a lightweight computational approach using XFLR5. The findings offer a practical methodology for early-stage design optimization of FW-VTOL UAVs, especially those operating at higher cruise speeds with piston engines.

ARTICLE INFO

Article History

Received: October, 2024

Received in revised form: January, 2025

Accepted: May, 2025

Published online: June, 2025

KEYWORDS

Aerodynamic Analysis, FW-VTOL UAV
Lift-to-Drag Ratio, NACA 4412, NACA 0011, XFLR5

INTRODUCTION

Unmanned Aerial Vehicles (UAVs) have rapidly evolved to address a diverse range of human needs, including surveillance, logistics, precision agriculture, and emergency response (Donatus et al., 2023; Rodríguez, Velastequí, 2019). Among these, fixed-wing vertical take-off and landing (FW-VTOL) UAVs have gained particular attention due to their ability to merge the vertical mobility of rotorcraft with the cruise efficiency of fixed-wing platforms (Blamis et al., 2021; Çakir & Kurtuluş, 2022). This hybrid capability enables operations in constrained environments without sacrificing range or endurance (Bustamante et al., 2019; Sonkar et al., 2023). Applications extend across civilian and military sectors, from search and rescue and environmental monitoring to urban air mobility and tactical reconnaissance (Kankanawadi et al., 2021; Sharma et al., 2021).

Despite their growing appeal, the design of FW-VTOL UAVs presents significant aerodynamic

challenges (Anuar et al., 2023). These platforms must operate efficiently in both vertical and horizontal flight modes, requiring careful consideration of stability, control, and transition dynamics. Key performance factors such as lift-to-drag ratio (L/D), wing geometry, and airfoil selection play a crucial role in maintaining efficiency during mode transitions (Dündar et al., 2020; Saengphet & Thumthae, 2017). Advanced control systems and optimized airframe designs are also needed to manage complex aerodynamic interactions and maintain stable flight throughout diverse operational regimes (Panigrahi et al., 2021; Prieto et al., 2023).

Traditionally, aerodynamic analyses for UAVs rely on either experimental testing or high-fidelity computational fluid dynamics (CFD) simulations using tools such as ANSYS Fluent and OpenFOAM (Prakoso et al., 2023). While these methods provide detailed insights, they are often prohibitively resource-intensive for early-stage design. Moreover, the extensive

Corresponding author: Dafiaghor Aghoghorohenena Gordon



Aerospace Engineering Department, Air Force Institute of Technology, Kaduna, Nigeria.

© 2025. Faculty of Technology Education. ATBU Bauchi. All rights reserved

computational time required can slow down design iteration, particularly for conceptual frameworks (Panigrahi et al., 2021; Zaharia et al., 2023).

To overcome these limitations, this study adopts XFLR5, a computationally efficient tool that leverages the Vortex Lattice Method (VLM) and Panel Methods for low-speed aerodynamic analysis. XFLR5 offers a practical trade-off between accuracy and speed, making it suitable for evaluating airfoils, wings, and full aircraft configurations at early design stages. Compared to CFD tools, XFLR5 enables quicker optimization loops while still capturing essential aerodynamic behavior, thereby facilitating performance-oriented conceptual design of FW-VTOL UAVs (Kyoung-Moo Min et al., 2019; Nugroho et al., 2022; Zaharia et al., 2023).

This study addresses a specific gap in existing literature: the lack of focused aerodynamic optimization for piston-engine FW-VTOL UAVs using computationally efficient tools. Most prior work either addresses general UAV aerodynamics or relies on resource-heavy CFD analyses. Here, we demonstrate how XFLR5 can be employed to optimize the L/D ratio and analyze aerodynamic efficiency across various trim and attack angles, specifically targeting enhancements in range and cruise performance. A key feature of this research is the comparative evaluation of airfoils. While the Eppler 66 airfoil is known for its high lift coefficient, it demonstrates greater sensitivity to small variations in angle of attack, which can lead to instability under dynamic flight conditions. In contrast, the NACA 4412 airfoil provides a higher L/D ratio at the UAV's design cruise speed of 25 m/s, resulting in improved stability and efficiency. For tail surfaces, the symmetric NACA 0011 airfoil was chosen to promote balanced control characteristics. This careful selection contributes to both aerodynamic performance and reliable flight control.

By integrating aerodynamic theory, computational modeling, and airfoil optimization, this work contributes a replicable framework for the efficient design of FW-VTOL UAVs, particularly in applications requiring extended

range and operational flexibility under piston-engine propulsion.

Hassan Alian et al. (2019), explored the conceptual design and optimization of a tilt-rotor micro air vehicle (MAV). The wing design, inspired by bat wings, featured dimensions including an estimated weight of 0.85 kg, wing loading of 3.46 kg/m², a surface area of 0.25 m², and an aspect ratio of 2.32. The resulting wingspan was 0.76 m. The 3D wing shape was generated and analysed using XFLR5 software, which also allowed for the visualization of lift, drag, and pressure distributions. A maximum lift-to-drag ratio of 18 was achieved at an angle of 1.8°, with a cruise speed of 20 m/s. In 2019, Min et al. (Kyoung-Moo Min et al., 2019), designed and tested a hybrid fixed-wing VTOL UAV named Duo Drone, with specifications including a mass of 4.2 kg, a wing surface area of 0.52 m², a wingspan of 2.2 m, and an aspect ratio of 9.3. Aerodynamic analysis was conducted using XFLR5, focusing on the wing and tail. The wings utilized the SG6043 airfoil, while the vertical and horizontal tail surfaces used the NACA0011 airfoil. Designed to operate at Reynolds numbers between 200,000 and 500,000, the UAV achieved a flight time of 51 minutes at 13 m/s and 100 m altitude. However, flight results deviated by 32% from endurance calculations due to unaccounted drag.

Another study conducted by Min et al. (Min et al., 2018), investigated the design and CFD analysis of a low-altitude VTOL UAV using XFLR5, ANSYS Workbench V14.5, and ICFM-CFD. XFLR5 was employed for wing shape design, weight center and neutral point prediction, and thrust system design. CFD analysis was performed with ANSYS Workbench V14.5, while ICFM-CFD generated the Hybrid Mesh (Hexa Mesh & Prism Mesh). Among three airfoils (NACA 4412, NACA 2412, and NACA 23012), NACA 4412 was selected due to its favourable pitching moment characteristics at various angles of attack, with a Reynolds number of 500,000. The V-tail, positioned 100 mm below the main wing, was designed to minimize wake interference from the motor and propeller. Drag increased noticeably at angles of attack above 10°, and the addition of the propulsion system resulted in a

Corresponding author: Dafiaghor Aghoghorghenena Gordon



Aerospace Engineering Department, Air Force Institute of Technology, Kaduna, Nigeria.

© 2025. Faculty of Technology Education. ATBU Bauchi. All rights reserved



reduction of the maximum lift coefficient from 0.52 to 0.48.

Studies conducted by Bustamante *et al.*, (Bustamante *et al.*, 2019), developed a VTOL UAV with a ducted-fan and tilt-rotor configuration, aiming to merge the hover capabilities of helicopters with the speed and load capacity of fixed-wing aircraft. Preliminary aerodynamic designs were conducted using XFLR5, while ANSYS Fluent® was employed for verifying the fixed-wing design. During flight testing, the UAV achieved a travel distance of 31.5 meters at a maximum altitude of 4 meters and operated for 20 minutes. In (Panigrahi *et al.*, 2021), the research presented the design of a hybrid VTOL tilt-rotor UAV to enhance endurance. The UAV featured a fixed-wing bi-copter with thrust vectoring, a wingspan of 1.10 meters, a wing chord of 0.30 meters, a wing area of 0.325 m², and a mass of 1.825 kg, with a wing loading of 5.61 kg/m² and an aspect ratio of 3.726. The airfoil used was DAE 51. Aerodynamic analysis with ANSYS assessed various angles of attack, while XFLR evaluated control surface deflections. Results indicated that an elevator-down configuration increased airfoil asymmetry, leading to higher lift and drag coefficients, and XFLR confirmed the effectiveness of control surfaces in fixed-wing mode.

Another studies conducted by Sharma *et al.*, (Sharma *et al.*, 2021), analyzed the TURAC tilt-rotor VTOL UAV using CFD techniques and XFLR5. The selected NACA 34112 airfoil, known for its high lift coefficient (0.45) and reflex camber, was tested with a wingspan of 5520 mm, wing area of 4.238 m², mass of 4713 g, wing loading of 1.124 kg/m², and various geometric parameters. Vortex Lattice Method (VLM) analysis showed that, at a Reynolds number of 322,330, the lift coefficient increased and drag decreased with higher angles of attack up to stall. At Reynolds numbers from 2×10^5 to 1×10^6 , lift increased proportionally, and drag decreased at higher Reynolds numbers. Winglets effectively reduced vortex formation, and higher-pressure coefficients were observed on the wing's front surface. In (Prieto *et al.*, 2023), A separate investigation by Prieto *et al.*, optimized VTOL drones using

winglets, focusing on blended winglets and raked wingtips. They examined nine raked wingtips configurations with sweep angles of 30°, 45°, and 55°, and taper ratios of 0.25, 0.35, and 0.4. The optimal configuration was SA = 30° and TR = 0.25, which reduced drag but had high bending. For blended winglets, 27 configurations were tested with cant angles of 45°, 60°, and 70°, winglet heights of 60 mm, 90 mm, and 120 mm, and taper ratios of 0.2, 0.3, and 0.4. The best configuration (CA = 70°, WH = 120 mm, TR = 0.3) reduced induced drag by 13.1% and total drag by 4.8%, improving efficiency by 5.1% and momentum by 2.4%. XFLR5 was validated against RANS, showing similar trends at a lower computational cost, beneficial for initial design phases.

Findings from recent investigation (Anuar *et al.*, 2023), discussed the design and aerodynamic analysis of a fixed-wing vertical-taking-off-and-landing (FW-VTOL) UAV with a maximum take-off weight (MTOW) of 5.2 kg being able to meet the required mission profile of achieving speeds of 14m/s at a cruise altitude of 120m with a total flight time of 30 minutes. The design had a wing configuration with the following dimensions; wing loading (W/S) of 9.545 Kg/m², wing area (S) of 0.544762 m², wing span(b) of 1.95 m, mean aerodynamic chord (\bar{C}) of 280 mm, chord root (Cr) of 300 mm, chord tip (Ct) of 220 mm, aspect ratio (AR) of 7 and taper ratio (λ) of 0.76. The design made use of a V-tail configuration having an area of 0.1745m², an angle of 38°, a span of 0.72m, a chord root (Cr) of 300 mm, and a chord tip (Ct) of 180 mm. XFLR5 was used to analyze the characteristics of three airfoils, namely the Eppler 66, NACA 4412 and S9000.

The Eppler 66 was selected as the most suitable airfoil due to the fact that it had the highest lift coefficient (0.8775) at an angle of attack of 30. Another study conducted by Adawy *et al.*, (Adawy *et al.*, 2023) , used XFLR5 for the selection and analysis of single element airfoils like the E423 and S1223 with Reynolds number equal to 500,000 at a cruise speed of 14 m/s. Both airfoils were deemed unsuitable due to their susceptibility to laminar stall at low Reynolds numbers, a behavior not accurately captured by XFOil.. For

Corresponding author: Dafiaghor Aghoghoroghenena Gordon



Aerospace Engineering Department, Air Force Institute of Technology, Kaduna, Nigeria.
© 2025. Faculty of Technology Education. ATBU Bauchi. All rights reserved

the analysis of a composite UAV for search and rescue, In (Zaharia et al., 2023), Analysis by Zaharia et al., used XFLR5 to obtain the maximum coefficient of lift and the maximum coefficient of drag. The airfoils used were the NACA 4415 for the wing and the NACA 0015 for the winglets and tail. Maximum coefficient of lift was observed to be 1.2, while the corresponding coefficient of drag was observed to be 0.06 (it increased to this point as the angle of attack was increasing), both of which occurred at an angle of attack of 12°.

Another work by Bhattarai et al. (2023) conducted an aerodynamic analysis of a Blended Wing Body (BWB) UAV using XFLR5, focusing on a design with the following key parameters: a wing loading of 8 kg/m², a maximum takeoff weight of 3 kg, wing area of 0.372 m², wingspan of 1.5 m, aspect ratio of 6, taper ratio of 0.15, root chord of 0.57 m, tip chord of 0.09 m, leading-edge sweep angle of 30°, and a dihedral angle of 3°.

Four airfoils were employed across the span to enhance aerodynamic efficiency and achieve a smoother planform transition. The MH78 airfoil was applied from the root to 0.22 m of the span, the S5010 airfoil from 0.42 m to the wingtip, and the MH80 airfoil was incorporated at the 0.33 m spanwise location for additional performance refinement. The NACA 0012 profile was used for the vertical fin. The aerodynamic simulations were performed using the Ring Vortex Method (VLM2) with fixed speed polar type at a velocity of 25 m/s. Results showed a maximum lift-to-drag (L/D) ratio of 17, occurring at a trim angle of 3.5°, indicating stable and moderately efficient flight characteristics for the BWB configuration.

A review of related studies reveals that UAVs within the weight range of 20 kg or less often exhibit low speeds. Given the target speed of 25 m/s for this study's design, the NACA 4412 airfoil is preferred over the Eppler 66 due to its greater stability, despite the latter's higher lift coefficient. To enhance range, a higher lift-to-drag ratio is necessary. This research aims to improve upon recent findings, where a lift-to-drag ratio of 17 was achieved at the trim angle of 3.5°.

Fundamental Aerodynamic Concepts

- a) **Angle of Attack:** The angle of attack (α) is defined as the angle between chord (c) and the relative wind defined as flow velocity (V_∞). Hence, α is also the angle between lift and normal force and between drag and axial force. The geometrical relation between these two sets of components is given by (Raja et al., 2023):

$$L = N \cos \alpha - A \sin \alpha \quad (1)$$

$$D = N \sin \alpha + A \cos \alpha \quad (2)$$

L: Lift force (N) — the component of the aerodynamic force perpendicular to the free-stream velocity

D: Drag force (N) — the component of the aerodynamic force parallel to the free-stream velocity

N: Normal force (N) — the component of the aerodynamic force perpendicular to the chord line of the airfoil

A: Axial force (N) — the component of the aerodynamic force parallel to the chord line

α : Angle of attack (degrees or radians) — the angle between the chord line and the free-stream velocity

- b) **Lift, Drag, & Lift-To-Drag Ratio:** Lift and drag are aerodynamic forces that act on the aircraft while it moves through the air. Lift is upwards force mostly generated by wings lifting the aircraft up while drag backwards force caused due to friction and aerodynamic pressure (Rodríguez, Velastequí, 2019). The equations for both forces are given below:

$$L = \frac{1}{2} \rho V^2 S C_L \quad (3)$$

$$D = \frac{1}{2} \rho V^2 S C_D \quad (4)$$

L: Lift force (N)

D: Drag force (N)

ρ : Air density (kg/m³)

V: Free-stream velocity (m/s)

S: **Wing reference area** (m²) — This is the projected planform area of the wing, used as a

Corresponding author: Dafiaghor Aghoghorghenena Gordon



Aerospace Engineering Department, Air Force Institute of Technology, Kaduna, Nigeria.

© 2025. Faculty of Technology Education. ATBU Bauchi. All rights reserved

reference to non-dimensionalize lift and drag coefficients.

C_L : Coefficient of lift (dimensionless)

C_D : Coefficient of drag (dimensionless)

The lift to drag ratio is one of the most important parameters of any aircraft design configuration (Rao, 2019). It is crucial as it determines how much that can be generated in response to the corresponding drag that is experienced. It is a key factor that influences the range, endurance and even the fuel efficiency of the design. It is denoted by L/D or C_L/C_D .

- c) **Pitching Moment:** The airfoil pitching moment is the moment produced by the airfoil, while the aircraft pitching moment is the total moment produced by the plane (Pellnäs & Sandeberg, 2021). The equation is given by:

$$M = \frac{1}{2} \rho V^2 S C_m \quad (5)$$

Where: M = Pitching moment, C_m = Coefficient of moment

The total pitching moments about the center of gravity must be zero at the operating point, which means that the aircraft coefficient of moment C_m must be zero at the operating point (Pellnäs & Sandeberg, 2021).

- d) **Reynolds Number :** The Reynolds number is physically a measure of the ratio of inertia forces to viscous forces in a flow and is one of the most powerful parameters in fluid dynamics (Raja et al., 2023). It is denoted by:

$$Re = \frac{\rho V c}{\mu} \quad (6)$$

Re: Reynolds number (dimensionless)

ρ : Air density (kg/m^3)

V : Free-stream velocity (m/s)

c : Chord length of the airfoil (m)

μ : Dynamic viscosity of air ($\text{kg/m}\cdot\text{s}$)

where; $\rho V c$ = inertia forces and μ = viscous forces
Reynolds number is also an indicator of the behavior of a flow in a thin region next to a body in a flow where viscous forces are dominant, determining whether that flow is well behaved

(laminar) or randomly messy (turbulent). This thin region is called the boundary layer (Valencia et al., 2020).

- e) **Trim Angle:** The trim angle is a necessary parameter when considering steady flight, especially during the cruise phase. It ensures that the aircraft maintains equilibrium by balancing aerodynamic forces and moments, which is crucial for optimizing fuel efficiency and stability.

Computational Fluid Dynamics (CFD)

Computational Fluid Dynamics (CFD) is a branch of fluid dynamics that provides a cost-effective method for simulating real flows through the numerical solution of governing equations (Valencia et al., 2020). This research will utilize CFD for analysis, specifically employing XFLR5 for 3D modeling and analysis. XFLR5 is a free tool designed for analyzing airfoils, wings, and planes at low Reynolds numbers (Min et al., 2018). It supports both 2D and 3D analysis.

The 2D and 3D analyses in XFLR5 employ the Panel Method and the Vortex Lattice Method (VLM), specifically VLM2, which is based on the Ring method. The Panel Method divides the surface into flat segments, treating each as a source or sink to calculate the flow field around an airfoil. This approach uses equations for velocity potential and stream function to describe the flow (Durmu, 2023). The Vortex Lattice Method models the airflow around an object using a grid of vortex filaments that represent the circulation of air, enabling the calculation of aerodynamic forces (Durmu, 2023).

METHODS AND MATERIAL

The methodology for aerodynamic analysis of the conceptual FW-VTOL UAV using XFLR5 is outlined below, detailing the process from airfoil selection to the analysis of the wing and tail components. Two airfoils were selected based on a literature review and analyzed using the Direct Foil Design tool and XFOIL Direct Analysis Tool: NACA 4412 for the wing and NACA 0011 for the tail. Figure 1 and Figure 2 show the NACA 4412 and NACA 0011 airfoils, respectively.

Corresponding author: Dafiaghor Aghoghorghenena Gordon



Aerospace Engineering Department, Air Force Institute of Technology, Kaduna, Nigeria.

© 2025. Faculty of Technology Education. ATBU Bauchi. All rights reserved

The analysis of these airfoils employs the Panel method as described in Section 2.2, with the

following steps detailed in the subsequent sections:

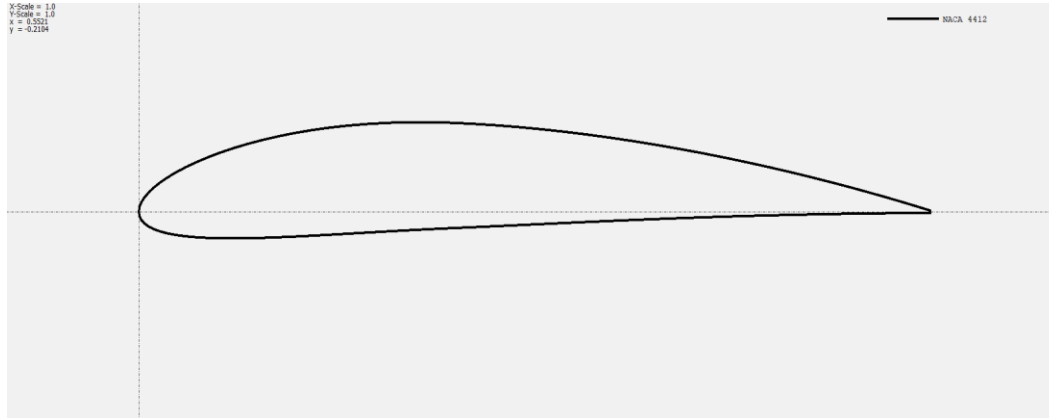


Figure 1 NACA 4412

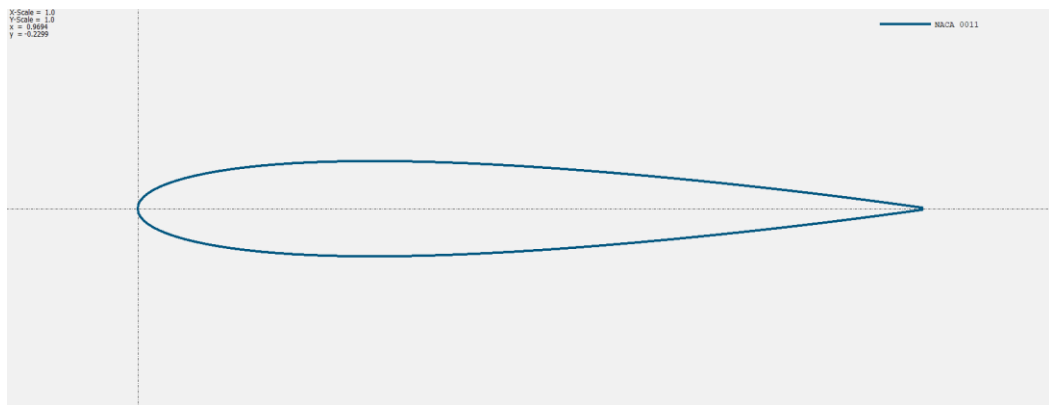


Figure 2: ACA 0011

Calculation of Reynolds Number

The Reynolds number for both the NACA 4412 and NACA 0011 is determined using Equation (6) and the following parameters:

$$Re = \rho Vc / \mu \quad (7)$$

$\rho = 1.095 \text{ kg/m}^3$, $V = 25 \text{ m/s}$, $c = \text{length of chord}$, $\mu = 1.543 \times 10^{-5} \text{ m}^2/\text{s}$

and 295,000. These values fall within the low-speed regime, validating the use of XFLR5's panel and vortex lattice methods for aerodynamic modeling. The differences in Reynolds numbers between components reflect variations in chord length, with the vertical tail generating slightly higher Reynolds numbers due to its longer chord. These results confirm that the airfoil selection and sizing are appropriate for efficient performance at the intended cruise speed.

As presented in Table 1, the calculated Reynolds numbers for the wing and tail airfoil sections range between approximately 269,000

Table 1. Reynolds Numbers Calculated for Each Airfoil Section at Cruise Speed (25 m/s)

Corresponding author: Dafiaghor Aghoghorghenena Gordon



Aerospace Engineering Department, Air Force Institute of Technology, Kaduna, Nigeria.

© 2025. Faculty of Technology Education. ATBU Bauchi. All rights reserved

	Airfoil Section	c	Re
NACA 4412	Wing section	0.153m	271,443,616
NACA 0011	Horizontal tail (elevator)	0.152m	269,669,475
NACA 0011	Vertical tail (Fin)	0.166m	294,507,453

Analysis of Airfoils

The airfoils are analyzed using the calculated Reynolds numbers and a range of angles of attack from -4° to 12° for both airfoils. The following figures illustrate the graphical analysis of the NACA 4412 and NACA 0011.

Figure 3 shows the graph of CL versus CD for the NACA 4412 wing airfoil, illustrating the

relationship between lift and drag coefficients. Figure 4 displays the graph of CL versus angle of attack for the NACA 4412 wing airfoil, highlighting how lift changes with varying angles of attack. Figure 5 presents the graph of CD versus angle of attack for the NACA 4412 wing airfoil, showing the variation in drag with different angles of attack.

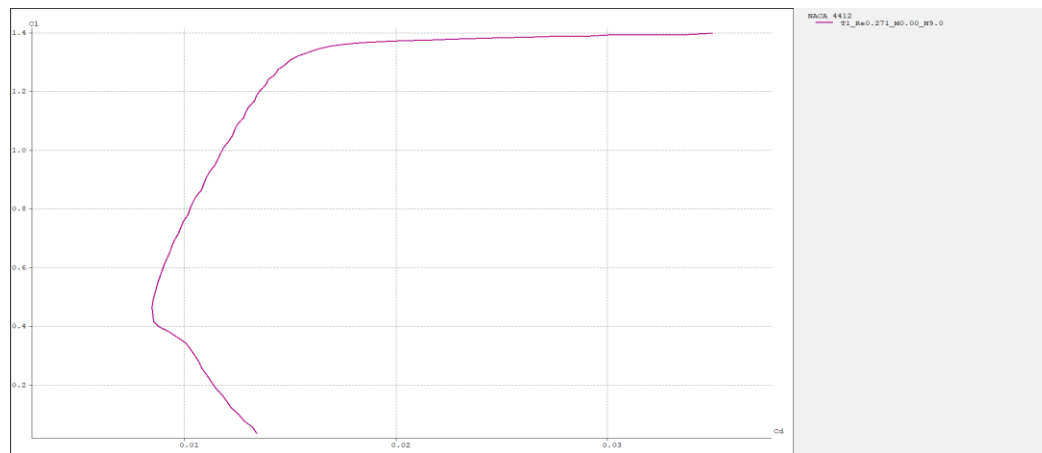


Figure 3. Graph of CL vs. CD for NACA 4412 (Wing Airfoil)

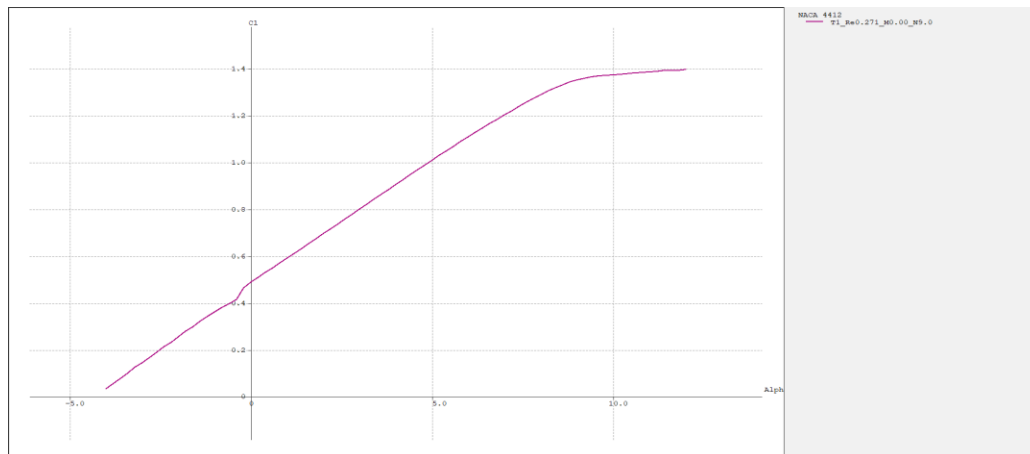



Figure 4. Graph of CL vs. Angle of Attack for NACA 4412 (Wing Airfoil)

Corresponding author: Dafiaghor Aghoghorghenena Gordon

 Aerospace Engineering Department, Air Force Institute of Technology, Kaduna, Nigeria.
© 2025. Faculty of Technology Education. ATBU Bauchi. All rights reserved

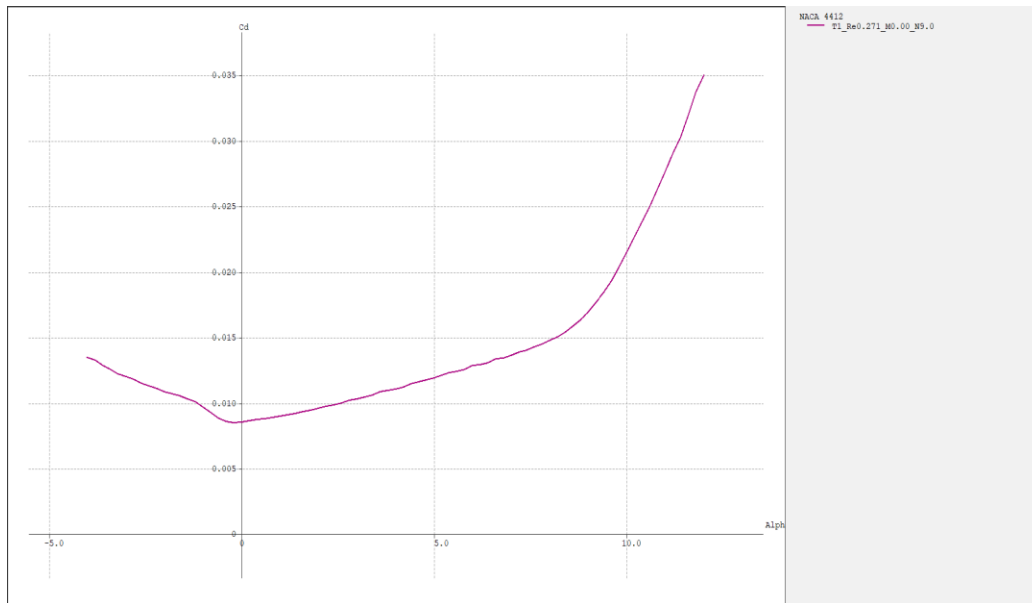


Figure 5 Graph of CD vs. Angle of Attack for NACA 4412 (Wing Airfoil)

Figure 6 depicts the graph of CL versus CD for the NACA 0011 elevator airfoil, indicating the lift-to-drag ratio. Figure 7 illustrates the graph of CL versus angle of attack for the NACA 0011 elevator airfoil, detailing how lift varies with angle

of attack. Figure 8 shows the graph of CD versus angle of attack for the NACA 0011 elevator airfoil, reflecting changes in drag as the angle of attack varies.

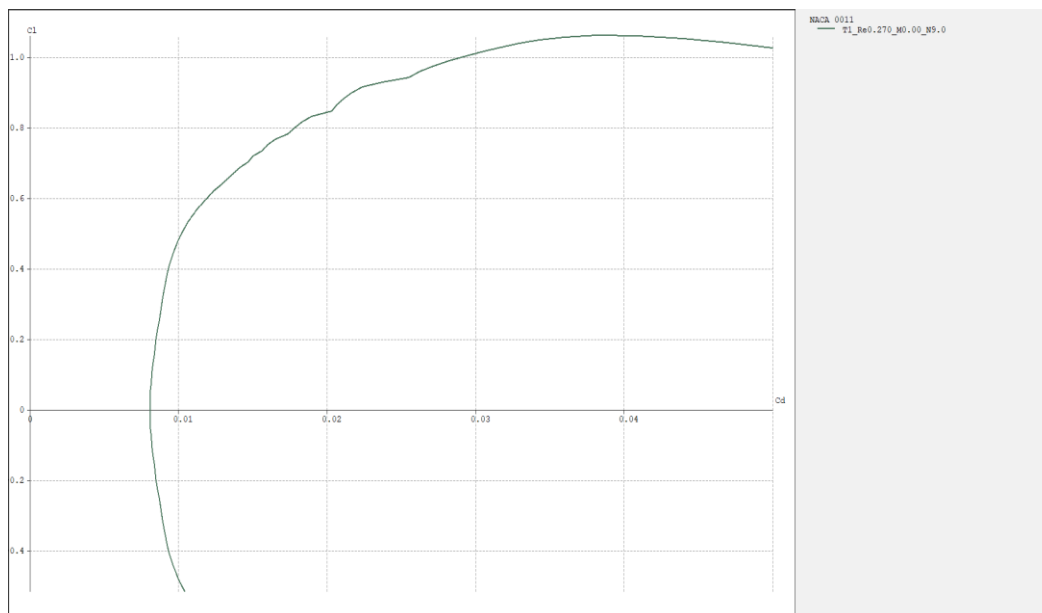


Figure 6 Graph of CL vs. CD for NACA 0011 (Elevator Airfoil)

Corresponding author: Dafiaghor Aghoghorghenena Gordon



Aerospace Engineering Department, Air Force Institute of Technology, Kaduna, Nigeria.
© 2025. Faculty of Technology Education. ATBU Bauchi. All rights reserved

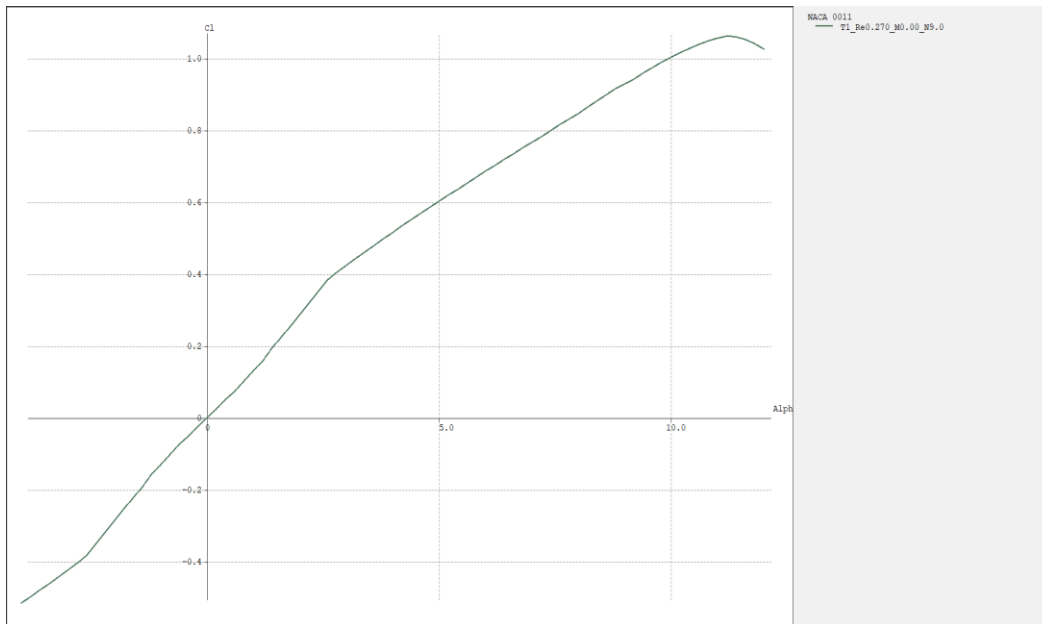


Figure 7 Graph of CL vs. Angle of Attack for NACA 0011 (Elevator Airfoil)

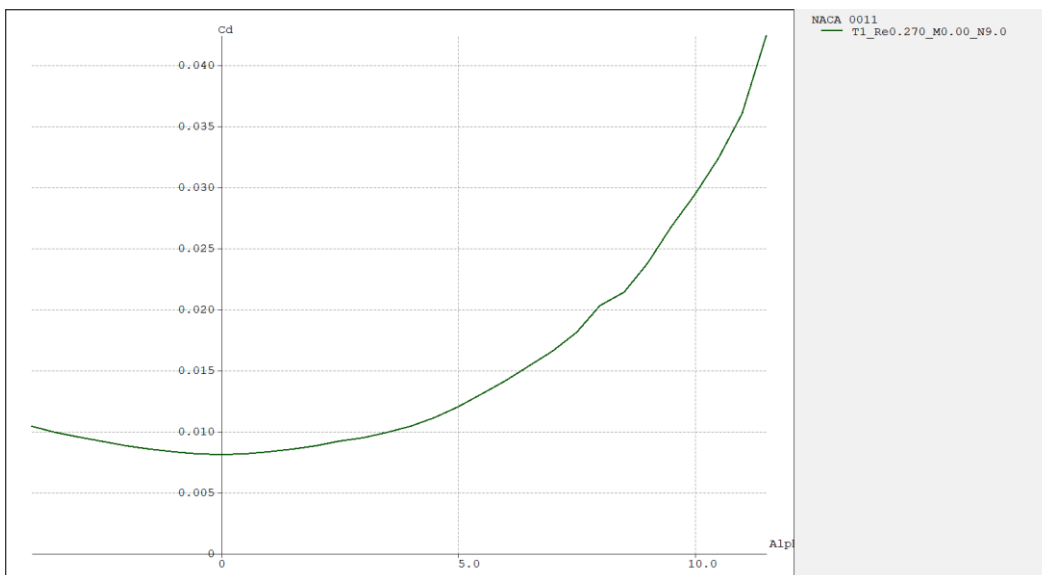


Figure 8 Graph of CD vs. Angle of Attack for NACA 0011 (Elevator Airfoil)

Figure 9 presents the graph of CL versus CD for the NACA 0011 fin airfoil, depicting the lift-to-drag relationship. Figure 10 illustrates the graph of CL versus angle of attack for the NACA 0011 fin airfoil, showing how lift changes with different

angles of attack. Figure 11 shows the graph of CD versus angle of attack for the NACA 0011 fin airfoil, demonstrating the effect of angle of attack on drag.

Corresponding author: Dafiaghor Aghoghorghenena Gordon



Aerospace Engineering Department, Air Force Institute of Technology, Kaduna, Nigeria.
© 2025. Faculty of Technology Education. ATBU Bauchi. All rights reserved

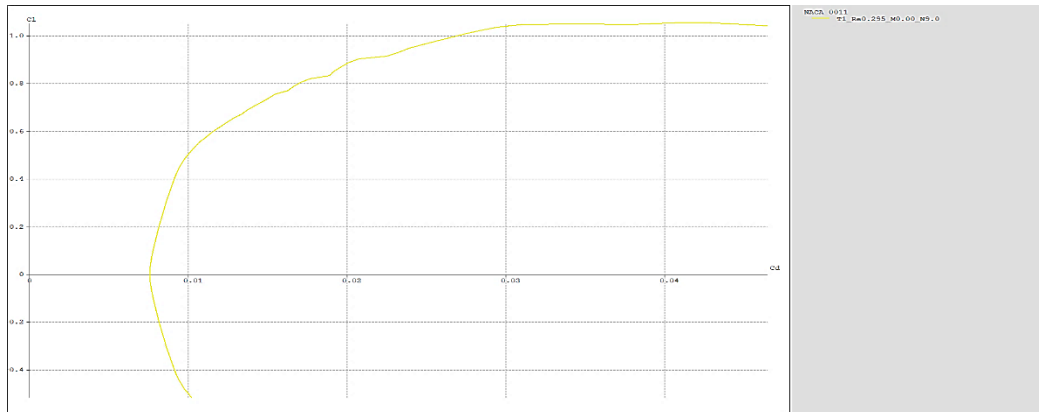


Figure 9. Graph of CL vs. CD for NACA 0011 (Fin Airfoil)

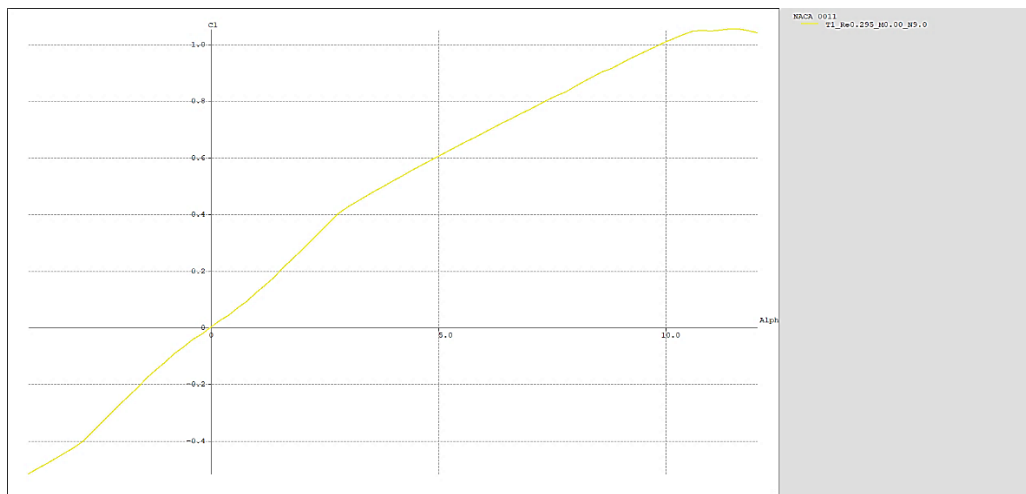


Figure 10. Graph of CL vs. Angle of Attack for NACA 0011 (Fin Airfoil)

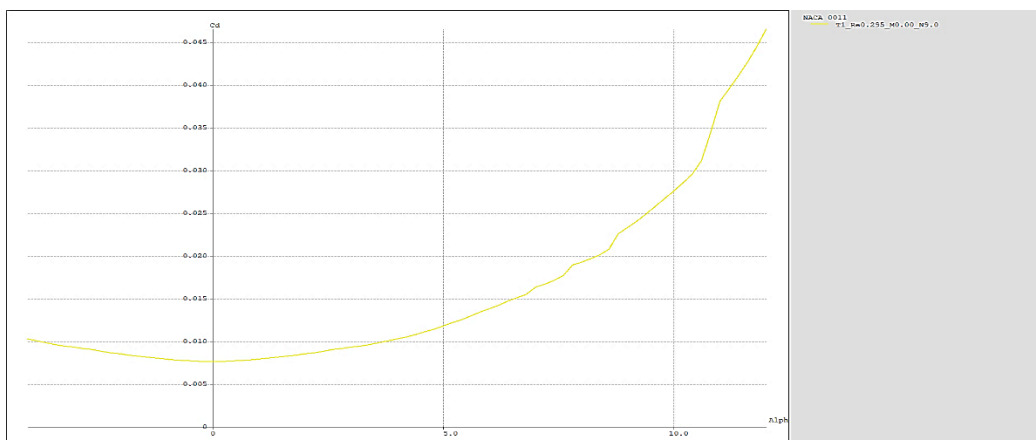


Figure 11 Graph of CD vs. Angle of Attack for NACA 0011 (Fin Airfoil)

Corresponding author: Dafiaghor Aghoghorghenena Gordon



Aerospace Engineering Department, Air Force Institute of Technology, Kaduna, Nigeria.

© 2025. Faculty of Technology Education. ATBU Bauchi. All rights reserved

Wing and Tail Model Design

XFLR5 facilitates model creation through the Wing and Plane Design tool. Utilizing this tool and the provided constraint data, the wing and tail models were developed. Table 2 outlines the key geometric and aerodynamic parameters used to construct the UAV model. The combination of a moderate aspect ratio ($AR = 9$), a relatively low taper ratio ($\lambda = 1$), and a cruise

speed of 25 m/s suggests a design optimized for aerodynamic efficiency and structural simplicity. The selected wing area and span support sufficient lift generation while maintaining stability through properly sized horizontal and vertical tail surfaces. These values guided the modeling process and enabled accurate performance prediction across different flight conditions.

Table 2 Aerodynamic and Geometric Design Parameters Used for Wing and Tail Configuration

S/no	Parameter	Value
1	Gross weight	20kg
2	Climb speed	13.65
3	Wing aspect ratio	9
4	Wingspan	1.383m
5	Wing chord	0.153m
6	Wing area	0.212m ²
7	Horizontal tail span	0.761m
8	Horizontal tail area	0.115m ²
9	Horizontal tail chord	0.152m
10	Vertical tail span	0.50m
11	Vertical tail area	0.08m ²
12	Vertical tail chord	0.166m
13	Taper ratio	1
14	Minimum Drag Coefficient C_{Dmin}	0.023
15	Cruise speed	25m/s

The required values from the table above were used to create the model of the wing

and tail. The Figures .12 to 15 below display the wing and tail model of the FW-VTOL

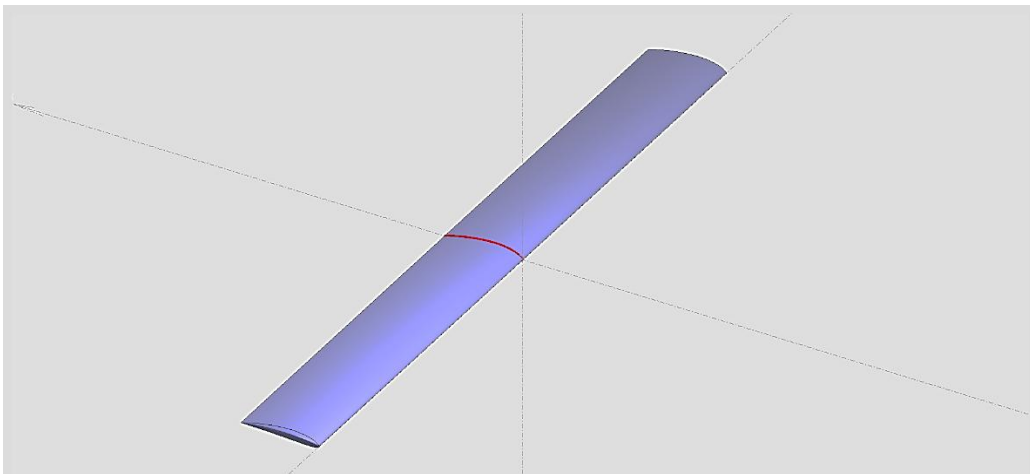


Figure 12. XFLR5 Model of the Wing

Corresponding author: Dafiaghor Aghoghorghenena Gordon



Aerospace Engineering Department, Air Force Institute of Technology, Kaduna, Nigeria.
© 2025. Faculty of Technology Education. ATBU Bauchi. All rights reserved

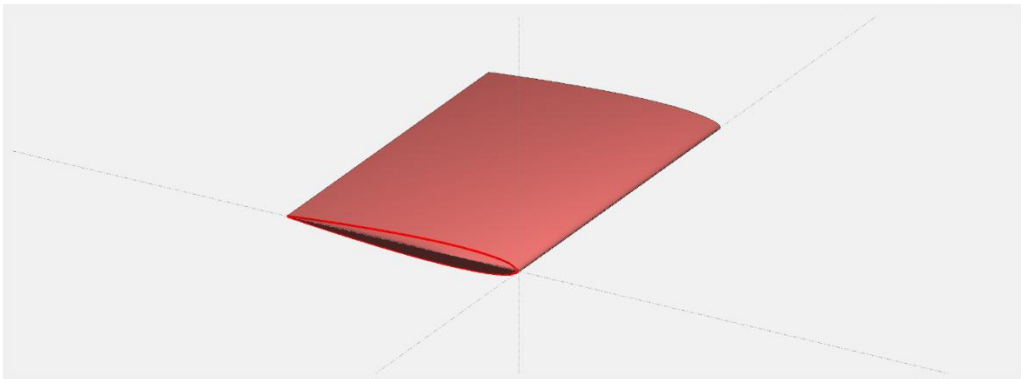


Figure 13. XFLR5 Model of the Fin

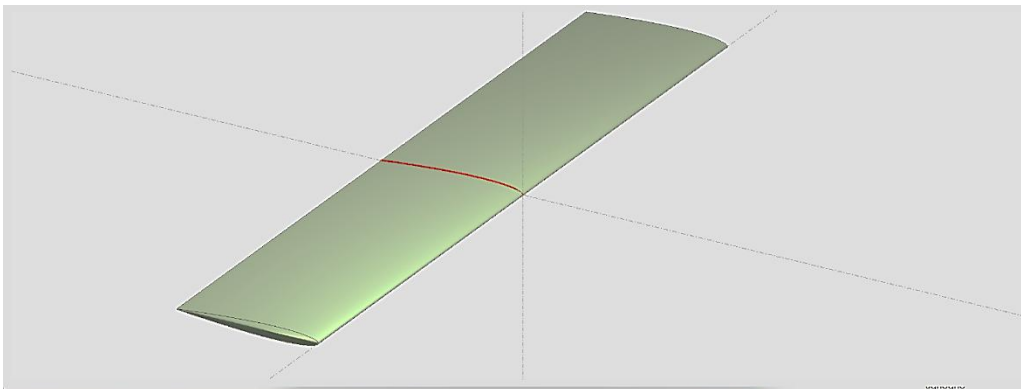


Figure 14. XFLR5 Model of the Elevator

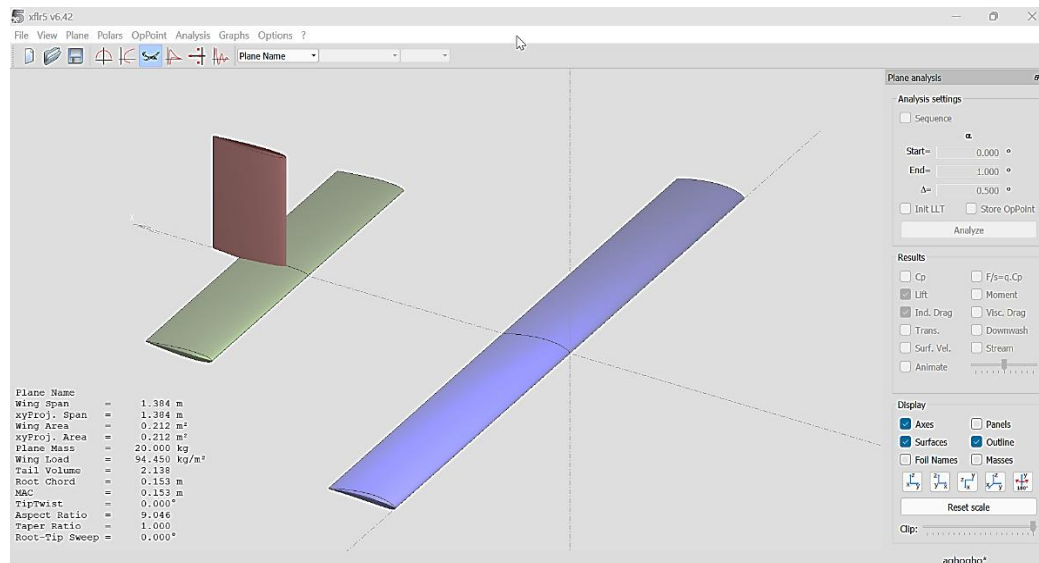


Figure 15. XFLR5 Models of the Wing and Tail

Corresponding author: Dafiaghor Aghoghorghenena Gordon



Aerospace Engineering Department, Air Force Institute of Technology, Kaduna, Nigeria.

© 2025. Faculty of Technology Education. ATBU Bauchi. All rights reserved

Analysis of Wing and Tail

The analysis of the wing and tail is done using the Ring method (VLM2) option of the XFLR5 software. The analysis was conducted with a fixed speed of 25m/s in a viscous flow and a selected angle of attack range of from 1° to 5° with an interval of 0.05°. The table 3 displays the necessary information for the analysis: The analysis settings summarized in Table 3 were selected to replicate steady-state cruise

conditions in a realistic operating scenario. By applying the Ring Method (VLM2) under viscous flow conditions at 25 m/s, the study ensured that aerodynamic behavior such as lift generation, drag buildup, and moment balance could be realistically simulated. These settings also align with prior UAV studies and facilitate meaningful comparison of aerodynamic performance metrics such as lift-to-drag ratio and trim angle.

Table 3. Analysis Settings Used for Wing and Tail Simulations Using XFLR5

Polar Type	Fixed Speed
Free Stream Speed	25m/s
Analysis Method	Ring Method (VLM2)
Flow	Viscous

RESULTS AND DISCUSSION

This section focuses on the results obtained from the methodology of the previous section.

Airfoil Discussion

Figure 16 shows the batch analysis of the NACA 4412 airfoil across various Reynolds numbers, illustrating how aerodynamic performance metrics vary with changes in flow conditions. The results help assess the airfoil's efficiency and stability under different operational scenarios.

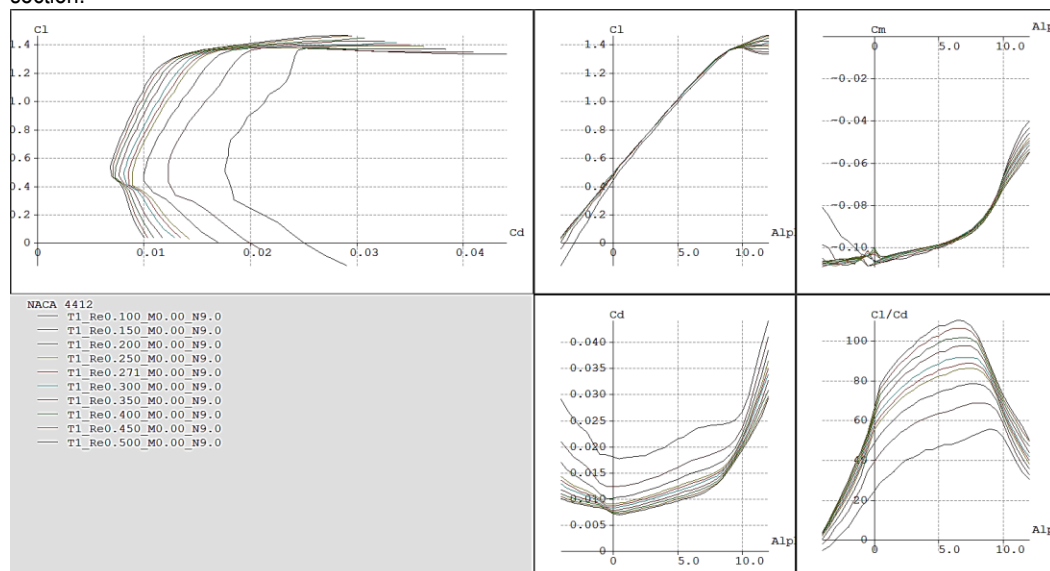


Figure 16. Batch Analysis of NACA 4412 at different Reynolds Numbers

Figure 17 presents the batch analysis of the NACA 0011 airfoil at various Reynolds numbers, highlighting changes in aerodynamic performance across different flow regimes. This

analysis provides insights into how Reynolds number variations affect the airfoil's lift and drag characteristics

Corresponding author: Dafiaghor Aghoghorghenena Gordon

Aerospace Engineering Department, Air Force Institute of Technology, Kaduna, Nigeria.
© 2025. Faculty of Technology Education. ATBU Bauchi. All rights reserved

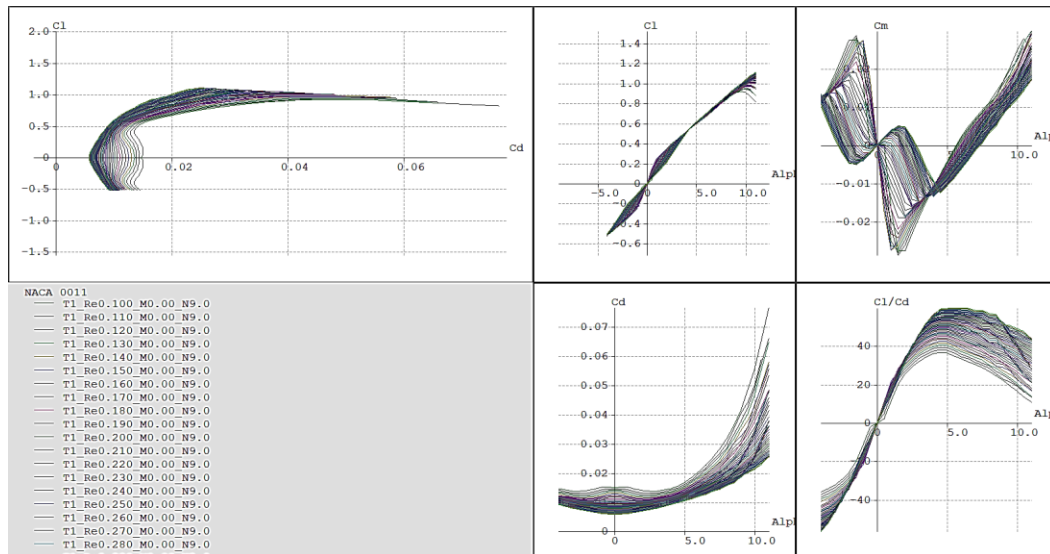


Figure 17. Batch Analysis of NACA 0011 at different Reynolds Number

The analysis of both airfoils shows that the NACA 4412 achieved a maximum lift coefficient (CL) of 1.4 and a corresponding CD of 0.035 at 12°. It is important to note that while the elevator and fin used the same airfoil (NACA 0011), both operated at different Reynolds number which resulted in slightly varying results for lift and drag. For the elevator, maximum CL observed to be 1.061 with a corresponding CD of 0.039 at 11.2°, while for the fin, maximum CL observed to be 1.053 with a corresponding CD of 0.042 at 11.53°. The NACA 4412 had negative pitching moments while the NACA 0011 had both negative and positive pitching moments. For both airfoils, after batch analyses at different Reynolds numbers, as the Reynolds number increased, lift increased proportionally while drag decreased, indicating improved aerodynamic performance at higher flow conditions.

Wing and Tail Analysis Results

Figures 18 to 22 illustrate the integrated configuration of the wing and tail assembly from multiple perspectives. Figure 23 provides four analytical plots: the Cl–Cd curve, the L/D ratio versus angle of attack, the Cd versus angle of attack, and the pitching moment (Cm) versus angle of attack. From the L/D vs. angle of attack

curve in Figure 3.8, the maximum lift-to-drag ratio (L/D) of 20.904 occurs between 3.05° and 3.10°, beyond which aerodynamic efficiency begins to decline due to increased drag. At the trim angle of 1.847°, the L/D ratio is 20.150, aligning with the desired condition for steady, level cruise at 25 m/s. The associated drag coefficient at this trim condition is 0.024, which closely approximates the theoretical minimum ($CD_{min} = 0.023$), validating the aerodynamic efficiency of the configuration. The pitching moment curve further confirms that the aircraft reaches equilibrium ($C_m \approx 0$) at this same trim angle, indicating a stable configuration without requiring excessive control input. This combination of high L/D and low pitching moment suggests effective aerodynamic balance.

In comparison to Bhattarai et al. (2023), who achieved a maximum L/D ratio of 17 at a trim angle of 3.5° for a Blended Wing Body UAV using XFLR5, the current study demonstrates superior aerodynamic performance. Specifically, the proposed design achieved a higher L/D ratio of 20.904 and a significantly lower trim angle of 1.847°, indicating a more aerodynamically efficient and stable configuration. These improvements are primarily attributed to the optimized selection of the NACA 4412 airfoil and the refined tail positioning strategy.

Corresponding author: Dafiaghor Aghoghorghenena Gordon



Aerospace Engineering Department, Air Force Institute of Technology, Kaduna, Nigeria.
© 2025. Faculty of Technology Education. ATBU Bauchi. All rights reserved

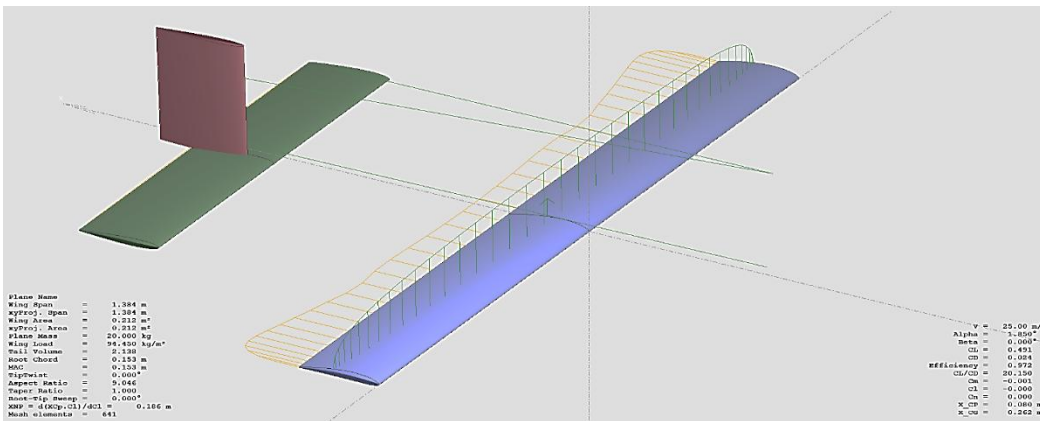


Figure 18. Aerodynamic Analysis in XFLR5

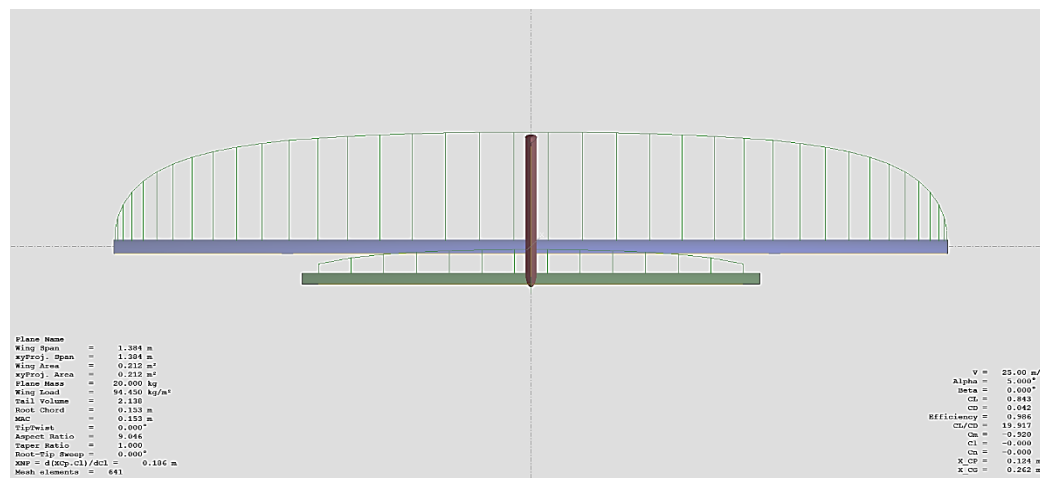


Figure 19. X-Plane Views of Wing and Tail

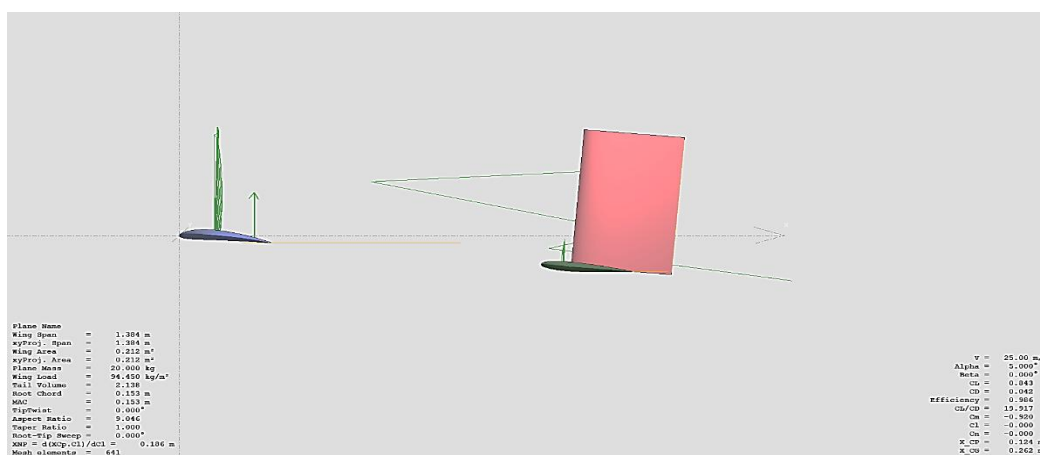


Figure 20. Y-Plane Views of Wing and Tail

Corresponding author: Dafiaghor Aghoghorghenena Gordon



Aerospace Engineering Department, Air Force Institute of Technology, Kaduna, Nigeria.

© 2025. Faculty of Technology Education. ATBU Bauchi. All rights reserved

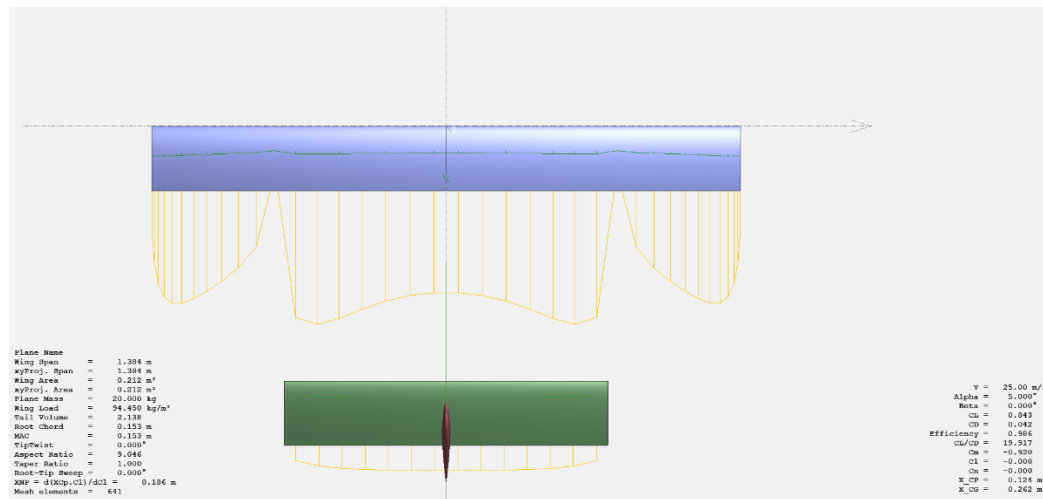


Figure 21. Z-Plane Views of Wing and Tail

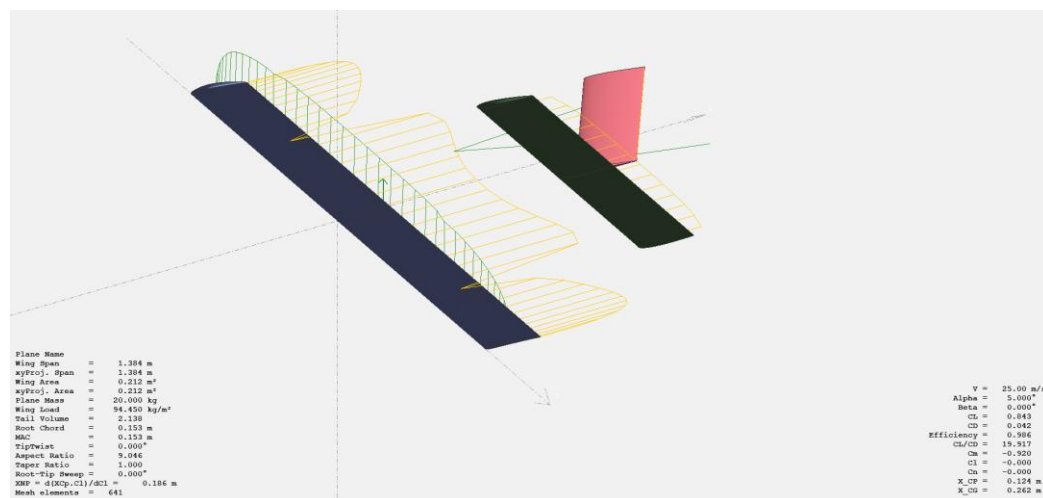


Figure 22. Flip Views of Wing and Tail

Following the analysis that was carried out and judging by the results presented in Figure 23 which comprises four distinct graphs, each providing insights into aerodynamic relationships. The first graph (top left) illustrates the relationship between the lift coefficient (C_L) and the drag coefficient (C_D), highlighting the optimal lift-to-drag ratio (L/D), which is further analyzed mathematically or through the second graph. The second graph (bottom left) depicts the variation of the lift-to-drag ratio (L/D) as a function of the angle of attack (α), demonstrating that at the trim angle

of 1.847° , the lift-to-drag ratio reaches 20.150. The third graph (top right) and the fourth graph (bottom right) show the relationship between the drag coefficient (C_D) and the angle of attack (α), as well as the relationship between the pitching moment (C_m) and the angle of attack (α), respectively.

The trim angle can be obtained from the graph of the pitching moment (C_m) plotted against the angle of attack (α). It is observed that the trim angle is 1.847° , meaning that steady flight occurs at this angle of attack. It is also noticed that at this

Corresponding author: Dafiaghgor Aghoghorghenena Gordon

Aerospace Engineering Department, Air Force Institute of Technology, Kaduna, Nigeria.
© 2025. Faculty of Technology Education. ATBU Bauchi. All rights reserved

angle, the coefficient of drag is 0.024 which is slightly above the calculated CD_{min} of 0.023. This

shows that the value obtained from the analysis is within the constraint parameters for the design.

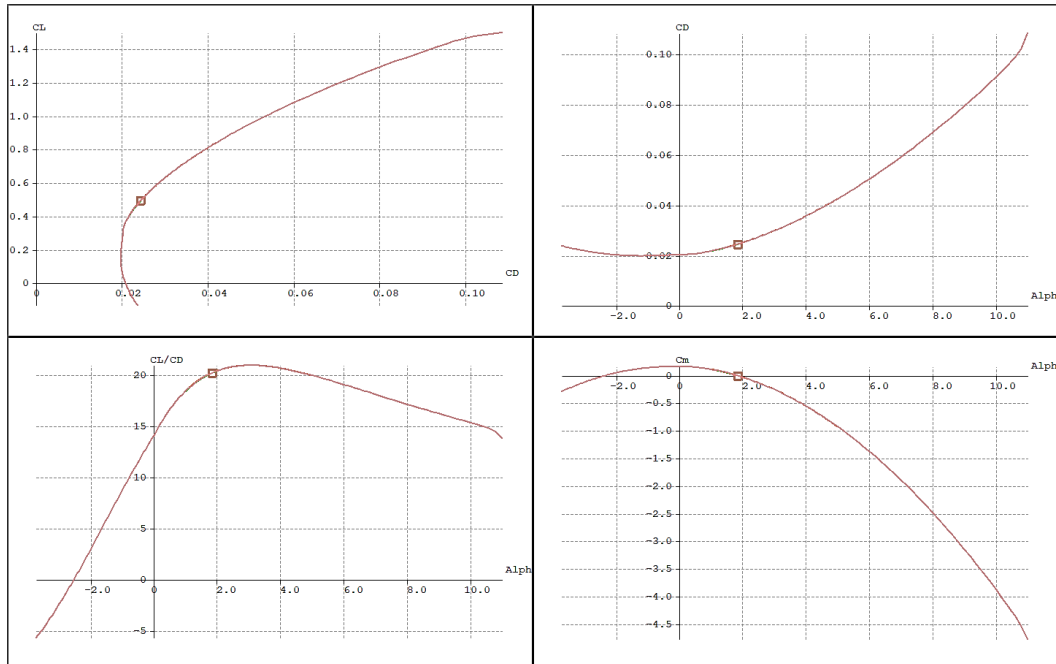


Figure 23. Graphical Results of Analysis

In addition, from Figure 23, It is observed that the maximum L/D ratio of 20.904 occurs at angles 3.05° and 3.10° , after which it starts to decrease following a further increase in the angle of attack. At the trim angle of 1.847° , the lift-to-drag ratio is 20.150 which mean that for steady flight at a fixed cruise speed of 25m/s, the ratio should be 20.150. As summarized in Table 4, both the lift-to-drag (L/D) ratio and pitching moment coefficient (C_m) show clear trends with increasing angle of attack. The maximum L/D ratio of 20.904 occurs between 3.05° and 3.10° ,

indicating the most efficient cruise condition. At a trim angle of 1.847° , the L/D ratio remains high (20.150), and the C_m value is close to zero, confirming longitudinal static stability. These aerodynamic characteristics support the effectiveness of the NACA 4412 airfoil and the tail positioning strategy in achieving a balanced and efficient flight configuration. This contrasts with Bhattarai et al. (2023), where a higher trim angle of 3.5° was needed for stable flight, indicating a less optimized aerodynamic setup.

Table 4. Variation of Lift-to-Drag Ratio and Pitching Moment with Angle of Attack

S/N	The angle of Attack ($^\circ$)	CL/ CD	CM
1	1.500	19.568	0.055
2	1.550	19.663	0.047
3	1.600	19.754	0.040
4	1.650	19.840	0.032
5	1.700	19.923	0.024
6	1.750	20.002	0.016

Corresponding author: Dafiaghor Aghoghorghenena Gordon



Aerospace Engineering Department, Air Force Institute of Technology, Kaduna, Nigeria.

© 2025. Faculty of Technology Education. ATBU Bauchi. All rights reserved



S/N	The angle of Attack (°)	CL/ CD	CM
7	1.800	20.078	0.008
8	1.850	20.150	-0.001
9	1.900	20.215	-0.009
10	1.950	20.278	-0.018
11	2.000	20.337	-0.027
12	2.050	20.392	-0.037
13	2.100	20.444	-0.046
14	2.150	20.493	-0.056
15	2.200	20.540	-0.066
16	2.250	20.584	-0.076
17	2.300	20.624	-0.086
18	2.350	20.662	-0.096
19	2.400	20.697	-0.107
20	2.450	20.727	-0.118
21	2.500	20.754	-0.129
22	2.550	20.780	-0.140
23	2.600	20.803	-0.151
24	2.650	20.823	-0.163
25	2.700	20.841	-0.175
26	2.750	20.856	-0.187
27	2.800	20.870	-0.199
28	2.850	20.881	-0.211
29	2.900	20.890	-0.224
30	2.950	20.897	-0.346
31	3.000	20.901	-0.249
32	3.050	20.904	-0.262
33	3.100	20.904	-0.276
34	3.150	20.902	-0.289
35	3.200	20.899	-0.303
36	3.250	20.894	-0.317
37	3.300	20.886	-0.331
38	3.350	20.877	-0.345
39	3.400	20.866	-0.359
40	3.450	20.853	-0.374
31	3.500	20.839	-0.389

CONCLUSION AND RECOMMENDATIONS

This study conducted a detailed aerodynamic analysis of a conceptual FW-VTOL UAV operating at a cruise speed of 25 m/s, focusing on lift-to-drag ratio (L/D) optimization and trim conditions. The trim angle for steady, level flight was identified as 1.847°, where the L/D ratio reached 20.150. At this condition, the drag coefficient was 0.024, closely matching the minimum drag value of 0.023, indicating high aerodynamic efficiency.

The analysis demonstrated an overall efficiency of 0.972, validating the aerodynamic configuration Compared to previous research by Bhattarai et al. (2023), where a Blended Wing Body UAV achieved a maximum L/D ratio of 17 at a trim angle of 3.5°, the present configuration shows a marked improvement, achieving an L/D ratio of 20.904 at a significantly lower trim angle of 1.847°. This discrepancy is primarily due to the aerodynamic advantages of the NACA 4412 airfoil, which offers a better lift-to-drag balance

Corresponding author: Dafiaghor Aghoghorghenena Gordon



Aerospace Engineering Department, Air Force Institute of Technology, Kaduna, Nigeria.

© 2025. Faculty of Technology Education. ATBU Bauchi. All rights reserved

and improved stability at the operating Reynolds number and cruise velocity of 25 m/s. Additionally, the linear configuration of the fixed wing and tail likely reduced interference drag compared to the blended wing planform. These improvements imply that conventional fixed-wing VTOL UAVs, when optimized with efficient airfoils and proper trim alignment, can outperform more complex geometries in cruise performance, especially in piston-engine UAV applications where power efficiency is critical.

Key findings include:

- 1) A maximum L/D ratio of 20.904 achieved between angles of attack 3.05° and 3.10° .
- 2) A trim angle of 1.847° corresponding to an L/D of 20.150.
- 3) A drag coefficient of 0.024 at trim, validating near-optimal cruise performance.
- 4) XFLR5 proved to be a reliable and efficient tool for early-stage aerodynamic design.

Recommended next steps for future research:

- 1) Wind tunnel testing to validate simulation results under real flow conditions.
- 2) Prototype fabrication to evaluate structural integrity and flight behavior.
- 3) High-fidelity CFD simulations (e.g., ANSYS Fluent or OpenFOAM) to capture detailed flow characteristics, particularly during transition between vertical and horizontal flight modes.

These actions will guide further refinement of the current design and accelerate the development of a fully functional FW-VTOL UAV capable of extended-range operations in real-world applications.

REFERENCES

- Adawy, M. El, Abdelhalim, E. H., Mahmoud, M., Ahmed, M., Mohamed, I. H., Othman, M. M., Elgamal, G. S., & Elshabasy, Y. H. (2023). Design and fabrication of a fixed-wing Unmanned Aerial Vehicle (UAV). *Ain Shams Engineering Journal*, 14(9), 102094.
<https://doi.org/10.1016/j.asej.2022.102094>
- Anuar, K., Fatra, W., Akbar, M., Nazaruddin, N., & Syafri, S. (2023). Design and Aerodynamic Analysis of Fixed-Wing Vertical Take-Off Landing (FW-VTOL) UAV. *Journal of Advanced Research in Fluid Mechanics and Thermal Sciences*, 1(1), 136–146.
- Bhattarai, R., Bhandari, N., & Sah, R. (2023). Aerodynamic design and analysis of a blended wing body UAV using XFLR5 [Master's thesis, Tribhuvan University]. TUCL eLibrary.
<https://elibrary.tucl.edu.np/items/0d98c742-c0aa-44ea-a96f-4866e25d0ad5>
- Bliamis, C., Zacharakis, I., Kaparos, P., & Yakinthos, K. (2021). Aerodynamic and stability analysis of a VTOL flying wing UAV. *IOP Conference Series: Materials Science and Engineering*, 1024(1).
<https://doi.org/10.1088/1757-899X/1024/1/012039>
- Bustamante, J. M., Herrera, C. A., Espinoza, E. S., Escalante, C. A., Salazar, S., & Lozano, R. (2019). Design and construction of a UAV VTOL in ducted-fan and tilt-rotor configuration. *2019 16th International Conference on Electrical Engineering, Computing Science and Automatic Control, CCE 2019*, 16.
<https://doi.org/10.1109/ICEEE.2019.8884533>
- Çakir, H., & Kurtuluş, D. F. (2022). Design and aerodynamic analysis of a VTOL tilt-wing UAV. *Turkish Journal of Electrical Engineering and Computer Sciences*, 30(3), 767–784.
<https://doi.org/10.55730/1300-0632.3810>
- Donatus, R. E., Dere, M. D., Donatus, I. H., Chiedu, U. O., Abdulrazaq, M. B., & Ohemu, M. F. (2023). Development of an Optimised Neural Network Model for RF Based UAV Detection and

Corresponding author: Dafiaghor Aghoghorghenena Gordon



Aerospace Engineering Department, Air Force Institute of Technology, Kaduna, Nigeria.
© 2025. Faculty of Technology Education. ATBU Bauchi. All rights reserved



- Identification. *Dutse Journal of Pure and Applied Sciences*, 8(4b), 82–91.
<https://doi.org/10.4314/dujopas.v8i4b.10>
- Dündar, Ö., Bilici, M., & Ünler, T. (2020). Design and performance analyses of a fixed wing battery VTOL UAV. *Engineering Science and Technology, an International Journal*, 23(5), 1182–1193.
<https://doi.org/10.1016/j.jestch.2020.02.002>
- Durmu, S. (2023). Aerodynamic Performance Comparison of Airfoils in Flying Wing Uav. *International Journal of Innovative Engineering Applications*, 7(1).
- HASSANALIAN, M., SALAZAR, R., & ABDELKEFI, A. (2019). Conceptual design and optimization of a tilt-rotor micro air vehicle. *Chinese Journal of Aeronautics*, 32(2), 369–381.
<https://doi.org/10.1016/j.cja.2018.10.006>
- Kankanawadi, N., Karinagshetru, G., Patil, L., Ultheru, B., Baruch, J., & Nallusamy, T. (2021). Conceptual design of a fixed wing vertical take-off and landing unmanned aerial vehicle. *AIP Conference Proceedings*, 2341(May).
<https://doi.org/10.1063/5.0050366>
- Kyoung-Moo Min et al., K.-M. M. et al. . (2019). Design , Flight Test Result of A Small Scale Hybrid VTOL UAV. *International Journal of Mechanical and Production Engineering Research and Development*, 9(2), 203–210.
<https://doi.org/10.24247/ijmperdapr201919>
- Min, K. M., Chia, F. Y., & Kim, B. H. (2018). Design and CFD analysis of a low-altitude VTOL UAV. *International Journal of Mechanical and Production Engineering Research and Development*, 9(2), 555–562.
<https://doi.org/10.24247/ijmperdapr201954>
- Nugroho, G., Hutagaol, Y. D., & Zuliardiansyah, G. (2022). Aerodynamic Performance Analysis of VTOL Arm Configurations of a VTOL Plane UAV Using a Computational Fluid Dynamics Simulation. *Drones*, 6(12).
<https://doi.org/10.3390/drones6120392>
- Panigrahi, S., Krishna, Y. S. S., & Thondiyath, A. (2021). Design, analysis, and testing of a hybrid vtol tilt-rotor uav for increased endurance. *Sensors*, 21(18), 1–21.
<https://doi.org/10.3390/s21185987>
- Pellnäs, A., & Sandeberg, J. (2021). Conceptual Design of a Small-Size Unmanned Air Vehicle Part A: Aerodynamic Performance and Structural Design. *Degree Project in Technology*.
- Prakoso, A., Pambekti, A., Budiono, C. S., Lukito, I., Kurniawan, R., & Vong, S. D. S. (2023). Perancangan dan analisis karakteristik aerodinamik pada pesawat fix wing VTOL UAV. *Angkasa: Jurnal Ilmiah Bidang Teknologi*, 15(1), 1.
<https://doi.org/10.28989/angkasa.v15i1.1373>
- Prieto, M., Escarti-Guillem, M. S., & Hoyas, S. (2023). Aerodynamic optimization of a VTOL drone using winglets. *Results in Engineering*, 17, 100855.
<https://doi.org/10.1016/j.rineng.2022.100855>
- Raja, V., Murugesan, R., Solaiappan, S. K., Arputharaj, B. S., Rajendran, P., Al-Bonsrulah, H. A. Z., Thakur, D., Razak, A., Buradi, A., & Ketema, A. (2023). Design, Computational Aerodynamic, Aerostructural, and Control Stability Investigations of VTOL-Configured Hybrid Blended Wing Body-Based Unmanned Aerial Vehicle for Intruder Inspections. *International Journal of Aerospace Engineering*, 2023.
<https://doi.org/10.1155/2023/9699908>
- Rao, S. S. (2019). *Conceptual Design of a Blended Wing Body Aircraft for Urban Air Mobility Operation Master's Final Degree Project*.

Corresponding author: Dafiaghor Aghoghorghenena Gordon



Aerospace Engineering Department, Air Force Institute of Technology, Kaduna, Nigeria.

© 2025. Faculty of Technology Education. ATBU Bauchi. All rights reserved



- Rodríguez, Velastequí, M. (2019). *DESIGN, MODELING AND CONTROL OF A HYBRID UAV*. September, 1–23.
- Saengphet, W., & Thumthae, C. (2017). Conceptual Design of Fixed Wing-VTOL UAV for AED transport. *The 7th TSME International Conference on Mechanical Engineering*, December, 1–12.
- Sharma, S., Sharma, R., Kumar, V., & Chandel, S. (2021). Analysis of a Tiltrotor Vertical Take-off and Landing Unmanned Aerial Vehicle: CFD Approach. *IOP Conference Series: Materials Science and Engineering*, 1116(1), 012096.
<https://doi.org/10.1088/1757-899x/1116/1/012096>
- Sonkar, S., Kumar, P., Puli, Y. T., George, R. C., Philip, D., & Ghosh, A. K. (2023). Design & Implementation of an Electric Fixed-wing Hybrid VTOL UAV for Asset Monitoring. *Journal of Aerospace Technology and Management*, 15(i).
<https://doi.org/10.1590/jatm.v15.1297>
- Valencia, E. A., Ayala, M. A., Hidalgo, V. H., Simbaña, S. F., Alulema, V. H., Rodríguez, D., & Cando, E. (2020). Aeropropulsive evaluation of boundary layer ingestion for medium electric-powered uavs. *AIAA Propulsion and Energy 2020 Forum*, September, 1–16.
<https://doi.org/10.2514/6.2020-3522>
- Zaharia, S., Pascariu, I. S., Chicos, L., Buican, G. R., Pop, M. A., Lancea, C., & Stamate, V. M. (2023). *Material Extrusion Additive Manufacturing of the Composite UAV Used for Search-and-Rescue Missions*.

